University of Dundee

Spectral matching and outdoor solar to electrical conversion efficiency in thin-film silicon multi-junction solar cells

Reynolds, Stephen; Urbain, F.; Smirnov, V.

Published in:
Journal of Physics: Conference Series

DOI:
10.1088/1742-6596/794/1/012025

Publication date:
2017

Document Version
Final published version

Spectral matching and outdoor solar to electrical conversion efficiency in thin-film silicon multi-junction solar cells

2017 J. Phys.: Conf. Ser. 794 012025

(http://iopscience.iop.org/1742-6596/794/1/012025)

IOP Conf. Series: Journal of Physics: Conf. Series **794** (2017) 012025 doi:10.1088/1742-6596/794/1/012025

Spectral matching and outdoor solar to electrical conversion efficiency in thin-film silicon multi-junction solar cells

S Reynolds[1], F Urbain[2,3] and V Smirnov[2]
[1] School of Science and Engineering, University of Dundee, Dundee DD1 4HN, Scotland.
[2] IEK-5 Photovoltaik, Forschungszentrum Jülich, D-52425 Jülich, Germany.
[3] Present address: IREC Catalonia Institute for Energy Research, Barcelona, Spain.

E-mail: s.z.reynolds@dundee.ac.uk

Abstract. Semi-empirical computer modelling is used to investigate spectral matching in tandem and triple-junction thin film silicon solar cells. In amorphous/microcrystalline silicon (a-Si:H/μc-Si:H) tandem cells, current mis-match is offset by an increase in fill-factor, resulting in a broad peak in efficiency versus average photon energy. For a-Si:H/a-Si:H tandem cells, photo-generated currents in both sub-cells increase with increasing average photon energy, and efficiency is predicted to increase monotonically over a wide spectral range. a-Si:H/a-Si:H/μc-Si:H triple cells exhibit spectral behaviour similar to a-Si:H/μc-Si:H tandem cells, but with a smaller fill-factor dependence. Variations in spectral quality are predicted to account for only a small reduction in annual electrical energy yield, of some 2 to 4%.

1. Introduction

Stacked multi-junction solar cells enable thermalisation and transmission losses to be reduced over the constituent single-junction cells, leading to an overall increase in photovoltaic conversion efficiency. This has been utilised in the development of multi-cell combinations of thin-film (amorphous and microcrystalline) silicon, yielding laboratory efficiencies of over 14% [1-4]. Further, increased terminal voltages (> 1.5 volts) are sufficient to drive photochemical water-splitting reactions directly, an application that has attracted considerable recent interest [5-7].

Careful matching of photogenerated currents is needed to optimise efficiency for a given spectrum [1,2], which in the laboratory is normally AM1.5G. However substantial variations in the solar spectrum occur naturally; multi-junction cells seldom operate outdoors in a current-matched condition, impacting on annual energy return. We present a model [8,9] that enables these effects to be evaluated. Realistic outdoor spectra are generated using a linear weighting function, and characterised in terms of average photon energy (*APE*) [10,11]. The short-circuit currents generated by sub-cells as a function of *APE* are calculated by numerical integration, and used to scale the J-V characteristics of reference single cells from which the overall J-V characteristic is obtained. Statistical distributions of spectral irradiance vs. *APE* are used to estimate long-term outdoor performance at a given location.

2. Experimental

2.1. Solar cell deposition

All cells were deposited in p-i-n superstrate configuration by plasma-enhanced chemical vapour deposition onto TCO coated glass. The top cell absorber layer of the a-Si:H/μc-Si:H tandem cell was

IOP Conf. Series: Journal of Physics: Conf. Series **794** (2017) 012025 doi:10.1088/1742-6596/794/1/012025

deposited at 180 °C with a silane concentration (SC) of 10%. For the a-Si:H/a-Si:H tandem cell and the a-Si:H/a-Si:H/μc-Si:H triple cell, the top a-Si:H absorber layer was deposited at 130°C with a SC of 4%, and the following a-Si:H layer at 180°C with a SC of 10%. Representative measured solar cell parameters are provided in table 1. Additional details are given elsewhere [2, 7].

Single junction 'reference' solar cells corresponding to top, middle and bottom were deposited under the same conditions. Layers representing the top, and (top + middle) sub-cells, used to filter the solar spectrum when measuring *J-V* characteristics of single cells representing the middle and bottom sub-cells, were deposited on glass slides and placed in the optical path.

Table 1. Representative measured cell parameters. V_{OC} is open-circuit voltage, J_{SC} short-circuit current, *FF* fill-factor and η conversion efficiency.

Cell configuration	a-Si/μc-Si	a-Si/a-Si	a-Si/a-Si/μc-Si
V_{OC} (V)	1.40	1.87	2.28
J_{SC} (mA/cm^2)	11.8	6.96	8.44
FF (%)	67.4	76.3	68.0
η (%)	11.1	9.9	13.1

2.2. Solar cell characterisation
Current–voltage (*J–V*) measurements under standard test conditions (100 mW/cm^2, 25°C) were made using a double source (Class A) AM1.5 sun simulator External quantum efficiency (EQE) measurements were conducted over the wavelength range 300 nm to 1100 nm using chopped light from a monochromator. Individual sub-cell EQEs of tandem and triple cells were determined separately, by using bias light sources to saturate those sub-cells not under measurement.

2.3 Modelling procedure
The modelling procedure has been described in detail elsewhere [8,9]. It consists of three main steps: (i) Solar spectra with *APE*s between 1.75 and 2.05 eV are generated by applying a linear spectral weighting function pivoted at 630 nm to the AM1.5 spectrum. The resulting spectra are similar in shape to those corresponding to a given *APE* [12,13]. (ii) The J_{QE} values for each sub-cell are calculated by numerical integration of the product of the EQE and a given spectrum, between 350 and 1050 nm. (iii) The relevant J_{QE} values are then used to shift each *J-V* curve along the current axis such that $J_{SC} = J_{QE}$. It is then straightforward to calculate points on the multi-junction *J-V* curve by adding the voltages for each sub-cell at the same current value.

3. Results and discussion

3.1. Sub-cell currents
The EQE data, from which J_{QE} values are computed for given model spectra, are presented in figure 1. The wavelength regimes over which each sub-cell generates photocurrent can be clearly identified. Figure 2 shows sub-cell currents vs. *APE* obtained when the solar spectrum is modelled for the three configurations studied here. The performance of multi-junction cells under given spectral conditions is constrained by the smallest of the currents generated by the component sub-cells. The a-Si:H/μc-Si:H tandem cell (figure 2(a)) is top-cell limited below *APE* = 1.90 eV, and bottom- cell limited above this. A peak in short-circuit current, of approximately 11.3 mA/cm^2 is predicted at around 1.90 eV. The a-Si:H/a-Si:H tandem cell (figure 2(b)) exhibits rather different behaviour. While the sub-cell currents are equal (around 7 mA/cm^2) at *APE* = 1.82 eV, the short-circuit current is predicted to increase monotonically with increasing *APE* over the range investigated. This is a consequence of differing

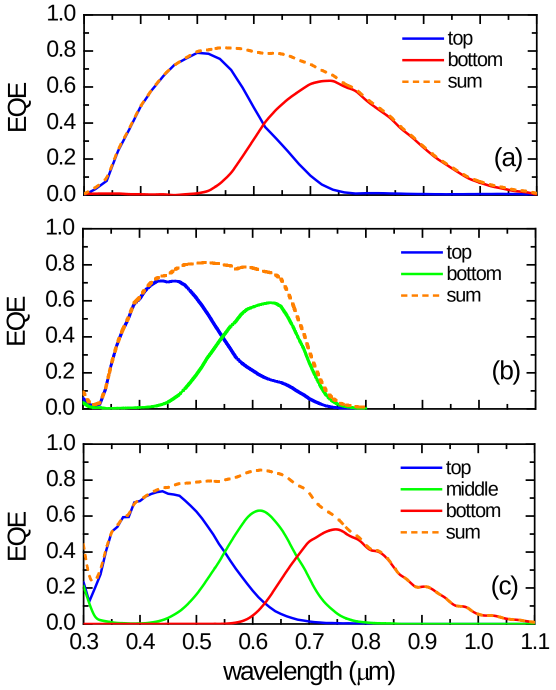

Figure 1. EQE measurements on: (a) a-Si:H/μc-Si:H tandem cell; (b) a-Si:H/a-Si:H tandem cell; (c) a-Si:H/a-Si:H/μc-Si:H triple cell.

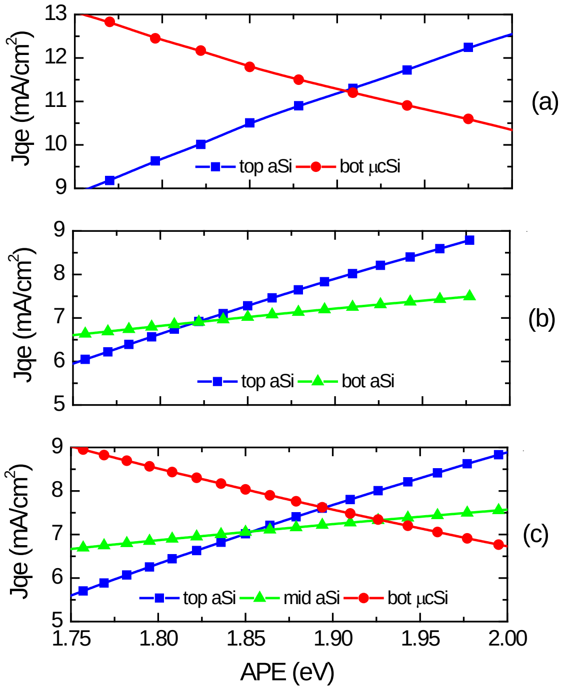

Figure 2. Modelled sub-cell currents for multi-junction cells: (a) a-Si:H/μc-Si:H; (b) a-Si:H/ a-Si:H; (c) a-Si:H/a-Si:H/μc-Si:H.

band-gaps of the bottom cells in these two cases, with the former requiring a thicker top-cell to generate sufficient current to achieve optimal matching

In the a-Si:H/μc- Si:H tandem cell, lower-energy photons generate a substantial fraction of the μc-Si:H bottom-cell current, as the higher-energy photons are absorbed by the thick (300 nm) top cell. This 'shadowing' causes the bottom-cell current to fall with increasing *APE*. In the a-Si:H/a-Si:H tandem cell however, the top cell is thinner (90 nm) and sufficient higher-energy photons are transmitted to the bottom-cell to increase the photogenerated current with increasing *APE*. As can be seen from figure 1(b), the a-Si:H bottom cell does not absorb significantly at wavelengths above 750 nm, so lower-energy photons have little bearing on performance of the a-Si:H/a-Si:H tandem. As *APE* increases beyond the range normally encountered outdoors, the a-Si:H bottom-cell current would ultimately begin to fall as the top-cell absorbs an increasing proportion of the total photon flux.

It can be seen from figure 2(c) that the a-Si:H/a-Si:H/μc-Si:H triple cell passes from top-cell limited to middle-cell limited (but still increasing short-circuit current) to bottom-cell limited (decreasing short-circuit current) as the *APE* is gradually increased. The triple-cell thus shares some of the properties of both tandem cells, but detailed behaviour will depend on layer thicknesses.

3.2 Fill-factor and efficiency

The variations in short-circuit current described in section 3.1 give a good indication of how the PV conversion efficiency of the tandem and triple cells will vary as a function of *APE*. However, while the open-circuit voltage does not vary greatly with *APE* [14], fill-factor may be quite strongly affected. Figure 3(a) reveals that *FF* increases significantly when the tandem cell becomes mismatched, particularly when bottom-cell limited, in agreement with [15]. This moderates the down-turn in efficiency when the short-circuit current decreases either side of the matching point. It should also be noted that the current-matched condition does not correspond exactly to the maximum-power condition. We have previously shown [9] that maximum power is predicted to occur when the tandem cell is mis-matched by 0.8 mA/cm^2, in favour of the top-cell. The a-Si:H/a-Si:H tandem cell (figure 3(b)) shows an increased *FF* when bottom-cell limited but a slight decrease when top-cell limited. Overall, efficiency increases quite strongly with increasing *APE*. The a-Si:H/a-Si:H/µc-Si:H triple-cell (figure 3(c)) simulation curves are similar to the a-Si:H/µc-Si:H tandem-cell, but *FF* variations are comparatively minor, leading to a narrower peak in efficiency. Figures 3(a) and 3(c) indicate that the power-matching for these cells occur at a bluer *APE* (1.93 eV) than the AM1.5G spectrum (1.88 eV).

3.3 Annual-average conversion efficiency

Figure 4 presents the PV conversion efficiencies of the three multi-junction cells as a function of *APE*. In order to determine whether these variations affect longer-term energy yield, a comparison between the efficiency curves and the annual-average spectral irradiance distribution must be made. This reveals variations in the position of the peak of the distribution depending on geographical location. A generic curve based on literature data has been added to figure 4 for comparison. For optimum annual energy yield, the peak in spectral irradiance distribution should be aligned with the peak in conversion efficiency. Figure 4 indicates that for the a-Si:H/µc-Si:H and a-Si:H/a-Si:H/µc-Si:H cells, the majority of the annual spectral irradiance is converted to electricity at a normalised efficiency of >98% of the peak value. More detailed calculations suggest that a 2-4% loss in annual energy due to spectral mis-match is a realistic estimate [9]. For the a-Si:H/a-Si:H cell there is no peak in efficiency, and provided the efficiency increases roughly linearly the gain at higher *APE* will tend to cancel the loss at lower *APE*. Thus spectral mis-match is predicted to have smaller impact in this case.

Figure 4 may be used to estimate the consequences of deploying cells or modules optimised for use at a specific value of *APE*, at a location where the most probable *APE* is not aligned with module peak efficiency. When the different spectral bandwidths are taken into account, distributions measured at a range of sites, including NREL (Colorado USA) [11,12], Ispra (Italy) [12], Loughborough (UK) [11]

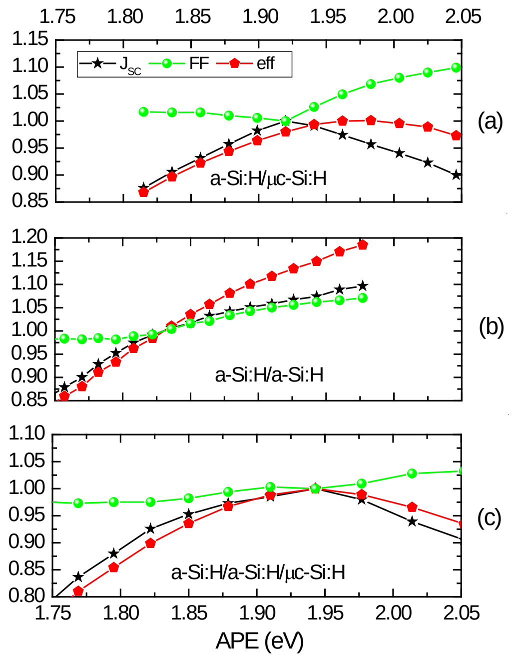

Figure 3. Modelled short-circuit current, fill-factor and efficiency for tandem and triple cells. All scales are normalised to 1.0 at the current-matched point.

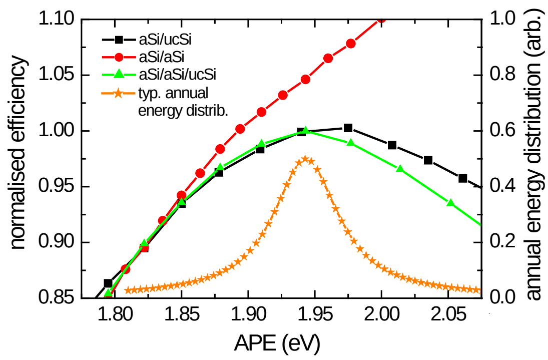

Figure 4. Modelled efficiencies for tandem and triple cells, normalised to overlap low-energy section of curves. Annual average irradiance distribution enables comparison.

and Kusatsu (Japan) [16] span a peak *APE* range of some 0.05 eV, similar to the widths of the distributions. For a tandem or triple cell matched for maximum efficiency under AM1.5G spectrum, the resulting variation in annual electrical energy production across these sites is of a similar magnitude to that due to the widths of the distributions.

Gottschalg et al [17] have differentiated band-gap effects and current mis-match effects for single and multiple cells, as 'primary' and 'secondary', respectively. Our model results indicate that the influence of these factors on long-term outdoor electrical output from multi-junction cells is complex. Spectral effects in multi-junction cells are generally minor compared with other site-related effects, such as temperature variations and degradation/annealing cycles [18], though some studies [19] suggest a greater significance.

3.4 Comparison of model predictions with laboratory and outdoor data

A number of the predictions made here, relating to variation of fill factor and the distinction between current-matching and power-matching, have been demonstrated in the lab for the case of a-Si:H/μc-Si:H tandem cells [14, 15, 20]. This supports the view that the approximations inherent in our model are not an over-simplification. Outdoor data are inherently quite noisy due to limitations in controlling or cancelling the influence of variables other than the set being studied, plus the non-unique nature of *APE* as a measure of spectral quality, which can make it challenging to identify trends. However, a peak in efficiency vs. *APE*, of a similar magnitude and profile to that predicted by our model, has been identified in outdoor test data from a-Si:H/μc-Si:H modules [16]. The tandem and triple-junction 'amorphous silicon' modules studied by Jardine et al [10] and Betts et al [11] behave quite similarly to our a-Si:H/μc-Si:H and a-Si:H/a-Si:H/μc-Si:H cells. Both show a peak in normalised current vs. *APE*, with that of the triple cell being more distinct, when compared with an amorphous silicon single junction. Krishnan et al [21] have performed modelling using actual spectra recorded in the Netherlands, for a-Si:H/a-SiGe:H/μc-Si:H triple cells. They have examined two cells, one well-matched to AM1.5G, and one poorly-matched. For the well-matched cell, the photogenerated current data agree quite well with our figure 3(c), although there are differences in detail, particularly regarding middle-cell current. This can be anticipated since the bandgap is smaller for the a-SiGe:H alloy than for our a-Si:H layer. Overall, results in the literature are in keeping with model predictions.

4. Conclusions

A semi-empirical model has been used to study the influence of solar spectral variations on current-matching in tandem and triple-junction thin film silicon solar cells, in terms of average photon energy. In a-Si:H/μc-Si:H tandem cells, current mis-match reduces photovoltaic conversion efficiency due to top-cell limitation at low *APE* and bottom-cell limitation at high *APE*. This is mitigated by an increase in fill-factor either side of the current-matched condition, resulting in a broad peak in efficiency vs. *APE* whose maximum occurs under slightly bottom-cell limited operation. As the majority of solar terrestrial spectral irradiance falls within a comparatively narrow *APE* range, within ±0.04 eV of the peak cell response, spectral variation is predicted to be a minor concern, accounting for a reduction in annual electrical energy yield of some 2 to 4%.

For a-Si:H/a-Si:H tandem cells, photo-generated currents in both sub-cells increase with increasing *APE* over the range of interest. The short-circuit current thus increases monotonically, with a reduction in gradient rather than a peak being observed at the current-matched point. *FF* is not strongly influenced, with a slight increase occurring under bottom-cell limitation. A peak in efficiency with *APE* is thus not anticipated for this combination. The model predicts that a-Si:H/a-Si:H/μc-Si:H triple cells will exhibit spectral behaviour similar to a-Si:H/μc-Si:H tandem cells, but with smaller variations in fill-factor. The modelled efficiency vs. *APE* peak is slightly narrower, leading to a greater (but still small) reduction in annual electrical energy yield than for the tandem cell.

Acknowledgments
The authors are grateful to K. Wilken for preparation of certain a-Si:H/a-Si:H cells used in this work, and to F. Finger for discussions.

References

[1] Yan B, Yue G, Sivec L, Yang J, Guha S and Jiang C 2011 *Appl. Phys. Lett.* **99** 113512
[2] Smirnov V, Lambertz A, Tillmanns S and Finger F 2014 *Can. J. Phys.* **92** 932
[3] Schüttauf J-W, Bugnon G, Stuckelberger M, Hänni S, Boccard M, Despeisse M, Haug F-J, Meillaud F and Ballif C 2014 *IEEE J. Photovoltaics* **4** 757
[4] Matsui T, Maejima K, Bidiville A, Sai H, Koida T, Suezaki T, Matsumoto M, Saito K, Yoshida I and Kondo M 2015 *Jpn. J. Appl. Phys.* **54** 08KB10
[5] Reece S Y, Hamel J A, Sung K, Jarvi T D, Esswein A J, Pijpers J J H and Nocera D G 2011 *Science* **334** 645
[6] Urbain F, Smirnov V, Becker J-P, Rau U, Ziegler J, Kaiser B, Jaegermann W and Finger F 2015 *Sol. Energy Mater. Sol. Cells* **140** 275
[7] Urbain F, Smirnov V, Becker J-P, Lambertz A, Yang F, Ziegler J, Kaiser B, Jaegermann W, Rau U and Finger F 2016 *Energy Environ. Sci.* **9** 145
[8] Reynolds S and Smirnov V 2012 *J. Phys.: Conf. Ser.* **398** 012006
[9] Reynolds S and Smirnov V 2015 *Energy Procedia* **84** 251
[10] Jardine C N, Betts T R, Gottschalg R, Infield D G and Lane K 2002 *Proc. 'PV in Europe – From PV Technology to Energy Solutions'* (Rome, Italy)
[11] Betts T R, Jardine C N, Gottschalg R, Infield D G and Lane K 2003 *Proc. 3rd World Conference on Photovoltaic Energy Conversion* (Osaka, Japan) p 1756
[12] Norton M, Gracia Amillo A M and Galleano R 2015 *Solar Energy* **120** 337
[13] Minemoto T, Nakada Y, Takahashi H and Takakura H 2009 *Solar Energy* **83** 1294
[14] Blank B, Ulbrich C, Merdzhanova Tz., Zahren C, Pieters B E, Gerber A and Rau U 2015 *Sol. Energy Mat. Sol. Cells* **143** 1
[15] Ulbrich C, Zahren C, Gerber A, Blank B, Merdzhanova Tz., Gordijn A and Rau U 2013 *Int. J. Photoenergy* **2013** 314097
[16] Minemoto T, Toda M, Nagai S, Gotoh M, Nakajima A, Yamamoto K, Takatura H and Hamakawa Y 2007 *Sol. Energy Mat. Sol. Cells* **91** 120
[17] Gottschalg R, Betts T R, Infield D G and Kearney M J 2005 *Sol. Energy Mat. Sol. Cells* **85** 415
[18] Gottschalg R, Betts T R, Eeles A, Williams S R and Zhu J 2013 *Sol. Energy Mat. Sol. Cells* **119** 169
[19] Virtuani A and Fanni L 2014 *Prog. Photovolt: Res. Appl.* **22** 208
[20] Bonnet-Eymard M, Boccard M, Bugnon G, Sculati-Meillaud F, Despeisse M and Ballif C 2013 *Sol. Energy Mat. Sol. Cells* **117** 120
[21] Krishnan P, Schüttauf J W A, van der Werf C H M, Houshyani Hassanzadeh B, van Sark W G J H M and Schropp R E I 2009 *Sol. Energy Mat. Sol. Cells* **93** 691